Tampere University

Tuomas Tinus

# PHOTOCATALYST PERFORMANCE EVALUATION THROUGH METHYLENE BLUE PHOTODECOMPOSITION

Faculty of Engineering and Natural Sciences
Bachelor of Science Thesis
May 2019

# ABSTRACT

Tuomas Tinus: Photocatalyst Performance Evaluation through Methylene Blue Photodecomposition
Bachelor of Science Thesis
Tampere University
Science and Engineering, BSc int. Degree Programme
May 2019

---

One widely used and effective way to measure the performance of a photocatalyst is indirectly with help of methylene blue, which readily photodecomposes in presence of a catalyst. Methylene blue is cheap and readily available from suppliers, and measuring its decomposition rate is simple due to its high absorbance in visible light range. Such indirect method does allow rapid iteration and improvement on existing photocatalysts by providing a way to qualitatively grade their efficiency without the need to go through i.e. complex water splitting measurement.

In this work, method for evaluation of performance of particulate photocatalysts based on photodecomposition of methylene blue is established. First, physics of light absorption and a method of determining concentration from light absorbance with Beer law is discussed, and methylene blue decomposition mechanism as well as experimental considerations reviewed. After that, equipment and methods for measurement of absorbance and determining methylene blue concentration are discussed. Then, research methodology, equipment and samples used are described, and finally results of the measurements and their analysis presented. The measured absorbance spectra during decomposition have deviated from the linear decrease predicted by theory, finding the source of the non-linearilty has, however, been left outside the thesis scope. A new model was developed, correlating the non-linear absorbance at 635 nm to concentration with help of a secondary absorption peak at 290 nm.

The final model for methylene blue decomposition shows reasonable agreement with theory, the decomposition profile is as Langmuir-Hinshelwood reaction mechanism predicts that of an exponential decrease. Catalysts under evaluation are clearly distinguished from each other, allowing the desired quantitative comparison between their activities which the method is designed to show. Core-shell catalyst with a photoactive layer of $TiO_2$ ALD grown on the surface of quartz particles at 100 °C is shown to have significantly lower photocatalytic efficiency than one with $TiO_2$ grown at 200 °C. However, significant error is clearly present in the low concentration range, which can in future work be eliminated by improving the calibration data set used to relate absorbance at 635 nm to methylene blue concentration and eliminating the original non-linearity source.To conclude, the method outlined in this work could effectively be used for quantitative comparison of photocatalyst activities of particulate photocatalysts and be used in research and development of photocatalyst materials.

Keywords: titania, photodecomposition, methylene blue, photocatalyst, ALD, titanium dioxide, solar fuels, spectrophotometry

# CONTENTS

# LIST OF FIGURES

# LIST OF ABBREVIATIONS AND SYMBOLS

## Acronyms

| | |
|---|---|
| $CO_2$ | carbon dioxide |
| $TiO_2$ | titanium dioxide |
| a.u. | arbitrary unit |
| ALD | atomic layer deposition |
| DI | de-ionized |
| IR | infrared |
| MB | methylene blue |
| NIR | near-infrared |
| PMT | photomultiplier tube |
| PTFE | polytetrafluorethylene |
| QP | quartz particle |
| RTA | rapid thermal annealing |
| TDMAT | tetrakis(dimethylamido)titanium |
| UV | ultraviolet |
| Vis | visible light |

## Glossary

| | |
|---|---|
| $A$ | absorbance |
| $A_0$ | absorbance at zero species concentration |

| | |
|---|---|
| $[A]$ | concentration of species $A$ |
| $c$ | concentration |
| $c_0$ | initial concentration |
| °C | degree Celsius, 0 °C = 273.15 K |
| $\epsilon$ | extinction coefficient |
| $E_{electronic}$ | electronic energy of a molecule |
| $E_{rotational}$ | rotational energy of a molecule |
| $E_{total}$ | total energy of a molecule |
| $E_{vibrational}$ | vibrational energy of a molecule |
| $I$ | light intensity |
| $I_0$ | initial light intensity |
| $k_{app}$ | apparent rate constant |
| $l$ | optical path length |
| nm | nanometer, 1 nm = $10^{-9}$ m |
| $Rate$ | rate of methylene blue decomposition |
| $\theta$ | surface site coverage |
| $t$ | time |
| $\mu$m | micrometer, 1 $\mu$m = $10^{-6}$ m |

# 1 INTRODUCTION

Out of the issues that humanity as a whole is globally facing, few are as critical as global warming and oil depletion. Levels of carbon dioxide and other greenhouse gases in the atmosphere keep rising due to human activity, and we are already starting to see consequences in form of increasing number of extreme weather events. In parallel, the unchanging dependency on oil for transportation and industrial production contrast with decreasing oil supplies and rising prices. One method, that is potentially key to solving both issues, is photocatalysis. A variety of chemical reactions using photocalysts and energy of the sun can i.e. be used to split water to produce hydrogen - effective fuel, which when burnt simply becomes water again, or to reduce carbon dioxide to produce so-called solar fuels - hydrocarbons that can be used as fuel or alternative source material for chemical industry in lieu of oil.

Developing efficient photocatalysts for water splitting and solar fuel production does require quick and straightforward methods for evaluating the performance of the catalysts. One widely used and effective way to do so is measuring performance indirectly with help of methylene blue, which readily photodecomposes in presence of a catalyst. Methylene blue is cheap and readily available from suppliers, and measuring its decomposition rate is simple due to its high absorbance in visible light range. Such indirect measurement does not allow for full evaluation of applicability of a catalyst to i.e. solar fuel production, due to the fact that it is not using the same reaction to measure efficiency. However, the method does allow rapid iteration and improvement on existing photocatalysts by providing a way to quantitatively grade their efficiency.

In this work, method for evaluation of performance of novel photocatalysts based on photodecomposition of methylene blue is established. First, physics of light absorption and a method of determining concentration from light absorbance is discussed, and methylene blue decomposition kinetics as well as experimental considerations reviewed. After that, equipment and methods for measurement of absorbance and determining methylene blue concentration are discussed. Then, research methodology, equipment and samples used are described, and finally results of the measurements and their analysis are presented.

# 2 PHYSICS OF LIGHT ABSORPTION

Light absorption in materials is central to measurement techniques and analysis done in this work, so the basic physical principles behind it need to be discussed. Absorption is one of the basic modes on light interaction with materials and is directly related to electronic structure of the material. Investigation of light absorption through a material allows determination of its composition.

In this chapter, connection of basic properties of materials to their absorption are discussed, building the theoretical foundation for the work discussed later.

## 2.1 Absorption and electronic structure

Absorption of light is directly related to electronic structure of materials. Absorption is defined as ”The conversion of the energy of electromagnetic radiation” ... ”into other forms of energy on passing through a medium” [1]. Because electromagnetic radiation is a form of energy, when it is absorbed it is converted into internal energy of the absorbing material. According to quantum theory, the amount of energy the molecule has is distributed as a series of discrete states, or levels as they are commonly called. We consider the total potential energy of a molecule of the material, which can be split into three different types of energy [2, p. 7]:

$$E_{total} = E_{electronic} + E_{vibrational} + E_{rotational} \tag{2.1}$$

The electronic energy is the energy of electrons on one electronic orbital or another [2, p. 7]. Molecules also posess vibrational energy, which corresponds to periodic stretching, bending or twisting (vibration) of the molecule, as well as rotational energy which corresponds to rotation of the whole molecule about some axis [2, p. 7]. Differences in energy of rotational and vibrational energy levels are 10 to 1000 times smaller than that of electronic energy levels [2, p. 7]. Rotational and vibrational energy levels can then be considered superimposed on the electronic levels, resulting in the energy level diagram as seen in Figure 2.1.

The exact values of energy level transition energies are very specific to molecules and their environment, such as presence of solvents and impurities. Indirect measurements - such as UV-visible absorption for determination of electronic level transition energies, therefore allow for determination of chemical composition and bonding in molecules [4,

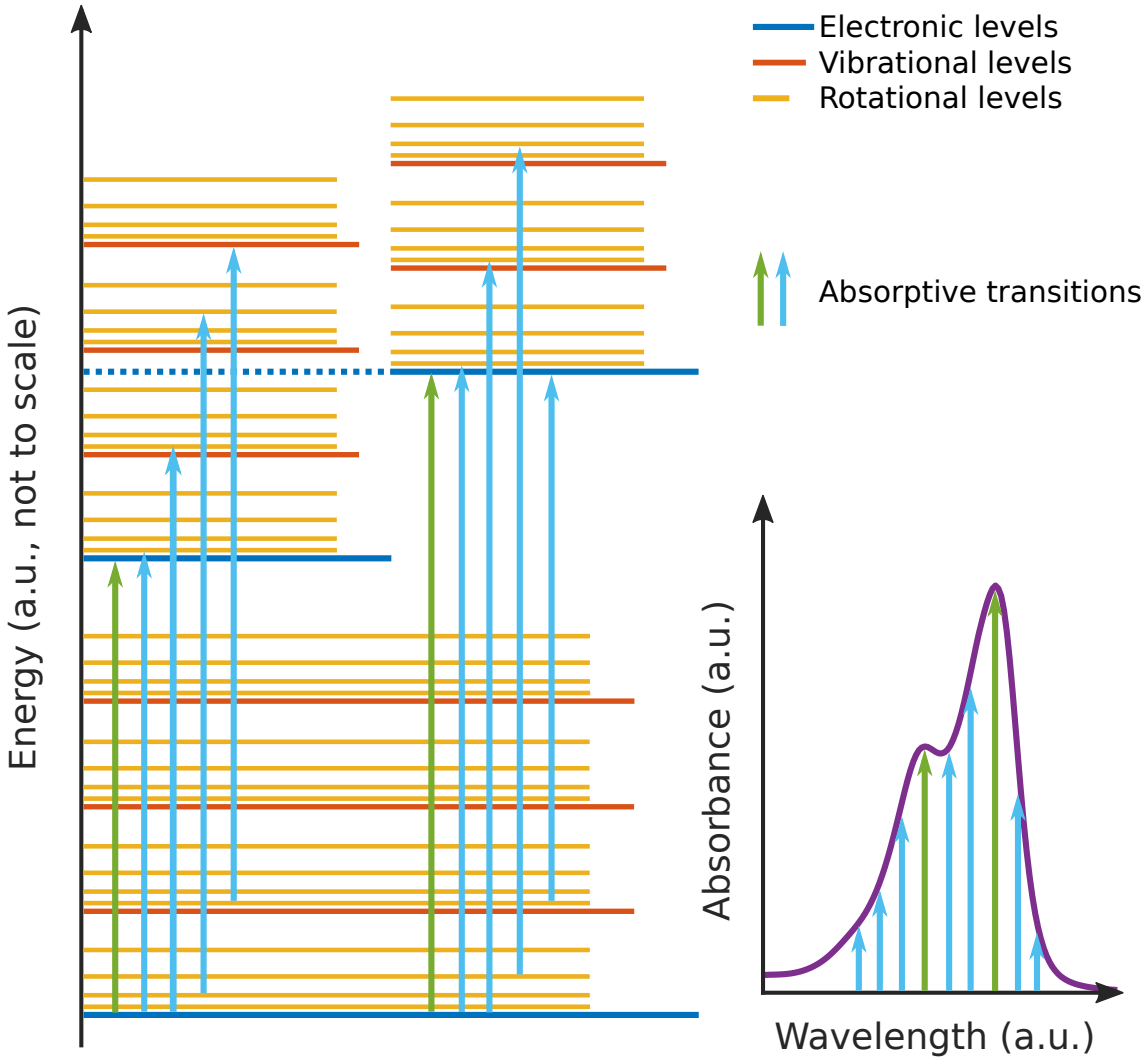


***Figure 2.1.*** *Molecular energy levels and transitions (adapted from [3])*

p. 49]. It must be noted, however, that in most cases the interpretation of absorbance spectra is more complex than described in this work, with many effects that can contribute to final spectrum shape - interaction of molecule with the solvent, Doppler broadening, etc. [2, p. 237-239].

## 2.2 Beer-Lambert law and concentration determination

In addition to determination of chemical composition, absorption measurements can be used for determining substance concentration. In this work, determination of concentration of an absorbing species in a solution is of most interest, so we consider Beer's law - a specialised form of Beer-Lambert law which relates concentration to transmittance through the sample [4, p. 49].

$$A = \epsilon c l = -log_{10}\left(\frac{I}{I_0}\right) \tag{2.2}$$

where $A$ is the absorbance, $\epsilon$ - the extinction coefficient of the absorbing species, $c$ - concentration of the absorbing species and $l$ - path length of light through the sample. In addition absorbance can be derived from transmittance - $I$ - the measured intensity trasmitted through the sample divided by $I_0$ - the measured intensity trasmitted through the sample in absence of the absorbing species. The extinction coefficient, as discussed eariler in this chapter, typically varies with respect to wavelength as it is based into light absorption in materials and so the material electronic structure. An equation can then be derived to extract concentration from transmitted intensity measurements:

$$c = \frac{-log_{10}\left(\frac{I}{I_0}\right)}{\epsilon l} = k * \left(-log_{10}\left(\frac{I}{I_0}\right)\right), \tag{2.3}$$

where $k$ is a coefficient, constant for a fixed path length, absorbing species and wavelength of light measured. It is straightforward, then, to derive $k$ from the extinction coefficient of a species found in literature and known path length, or experimentally by measuring transmission through a series of samples of known concentrations.

In some cases, it is desirable to measure $I_0$ in complete absence of the sample. The medium in which the absorbing species is contained itself typically absorbs some of the incoming light, in which case the equation takes the following form:

$$c = k * \left(-log_{10}\left(\frac{I}{I_0}\right) - A_0\right), \tag{2.4}$$

where $A_0$ is the absorbance at zero concentration of the desired absorbing species. This form still gives a linear dependence of concentration on absorbance, leaving a fixed offset of $k * A_0$ to be determined experimentally.

# 3 METHYLENE BLUE PHOTODECAY

Methylene blue, also known as methylthioninium chloride, is a medication and dye, first prepared in 1876 by Heinrich Karo [5]. Methylene blue is an ionic compound, with cation having a polycyclic structure of two benzene-like rings, one with an amino-group and one with a imine group, fuzed to a central 1,4-thiazine ring (Figure 3.1). The anion in methylene blue is the chloride ion.

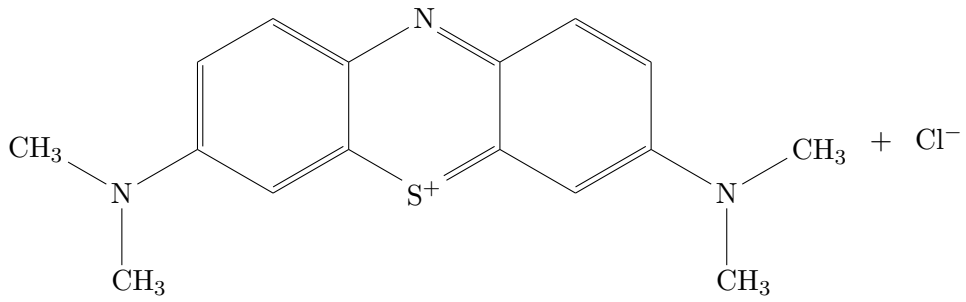


***Figure 3.1.*** *Chemical structure of methylene blue, adapted from [6]*

In this chapter, basics of interaction of light with methylene blue solutions are examined, as well as methylene blue photocatalytic decomposition and its chemical kinetics.

## 3.1 Interaction of methylene blue with light

The vibrant blue colour of methylene blue has ensured active use through the years - first as a stain in cell and tissue analysis, as first applied by Paul Ehrlich [5] and more recently as a model dye pollutant [7] and photocatalytic decomposition target [8]. One of the reasons for such active use as well as one of its consequences is the fact that a lot of research was done on the interaction of methylene blue with light. Methylene blue absorbs light strongly in even small concentrations, and the dependence of absorbance on concentration is linear, which allows the concentration to be easily determined. Example absorbance spectra of varying concentrations of methylene blue are shown in the following Figure 3.2:

In the spectra above, a number of features can be identified. Methylene blue absorbs light in a number of specific bands (peaks), depending on the exact concentration of methylene blue, presense or absence of other compounds in the solution, adsorption to other compounds, etc. The main methylene blue absorption peak is situated at 665 nm[9] and the related secondary peak at 290 nm[10]. Another commonly observed peak is that

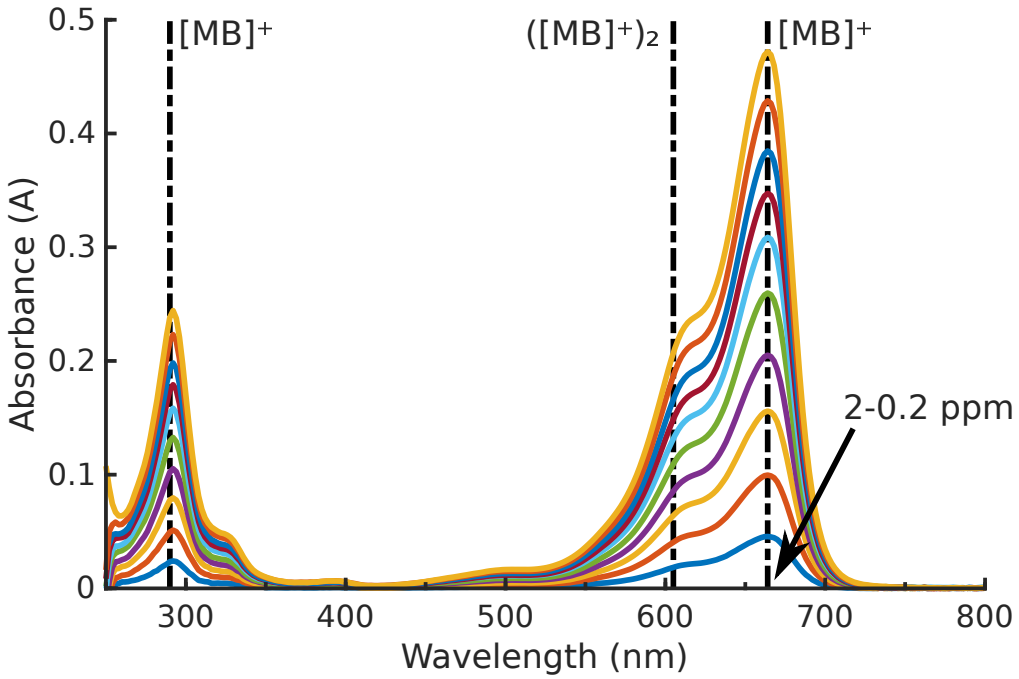


***Figure 3.2.*** *Absorbance spectra of pure MB solutions of concentration 0.2-2 ppm in 0.2 ppm steps (spectra measured as described in chapter 6). Marked absorption peak positions from literature [9, 10]*

of a methylene blue dimer $([MB]^+)_2$ at 605 nm[9] and in some conditions also methylene blue trimer $([MB]^+)_3$ at 580 nm[11].

## 3.2 Photodecomposition

Photodecomposition, also known as photodegradation or photolysis, is a process of decomposition of a substance due to the action of light [12]. While some materials degrade naturally in presence of light, using specifically-tailored photocatalyst materials photodecomposition is possible for materials that are normally stable in presence of light as well. In this work, photodecomposition of methylene blue in presence of a catalyst is used as a means to evaluate the efficiency of said photocatalyst.

The process of photodecomposition of methylene blue in aqueous solutions has been thoroughly documented [6, 13, 14]. In brief, the absorption of photons by the catalyst ($TiO_2$) produces pairs of negatively charged electrons in its conduction band and holes in its valence band [14]. Those act in a chain of chemical processes, ultimately resulting in oxidative reactions between organic reactants and either photogenerated holes or $OH\cdot$ radicals [6]. The oxidative processes described result in stepwise degradation of methylene blue. The final products of the process are almost exclusively $CO_2$, $NH_4{}^+$, $NO_3{}^-$ and $SO_4{}^{2-}$ [6]. Literature shows that methylene blue undergoes slow degradation in absence of catalyst under UV illumination, however that process is much slower than photodecomposition in catalyst presence [6].

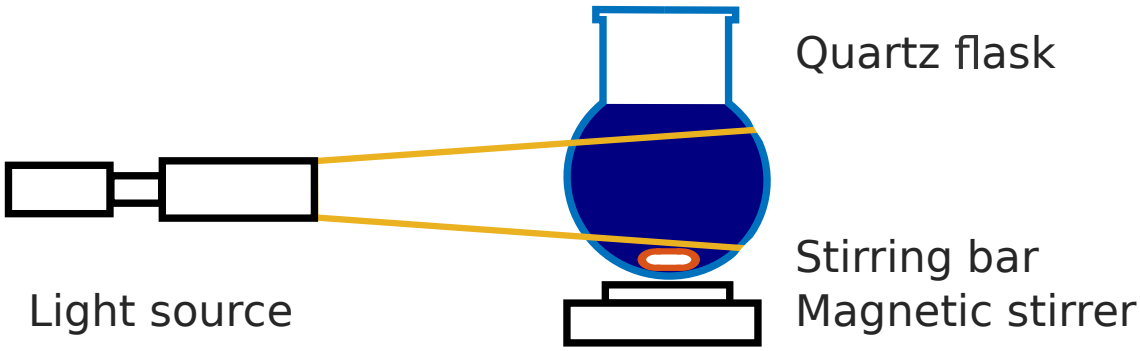


***Figure 3.3.*** *Diagram of a light exposure setup as used in this work*

An experimental setup for repeatable light exposure of methylene blue - catalyst aqueous solutions is presented in Figure 3.3. The setup includes: the light source, affixed at a preset distance from the round-bottom flask with the solution, a quartz round-bottom flask with the solution, a magnetic stirrer and PTFE-coated stirring bar for continued agitation of the solution as otherwise the catalyst would settle at the bottom. The whole setup is then typically shielded from external light inside an enclosure, as the methylene blue solution is sensitive to light.

As this work concerns chiefly titanium dioxide-based photocatalysts, some remarks need to be made with respect to their specificities. Specifically, $TiO_2$-based photocatalysts are typically most active in the UV wavelength range due to their large bandgap, and a large fraction of research in the area is targeting the extension of $TiO_2$-based photocatalyst activity into visible light range [15, 16, 17]. That precludes the usage of a light source with a spectrum that includes a significant proportion of UV-light, as well as i.e. round-bottom flasks made of quartz which, unlike plain borosilicate glass, have high transmittance in the UV range.

## 3.3 Methylene blue photodecomposition kinetics

Methylene blue photodecomposition in water solutions with $TiO_2$ as catalyst is commonly considered to follow the Langmuir – Hinshelwood mechanism in first order [6]. Langmuir – Hinshelwood mechanism is Hinshelwood's extension of Langmuir's theory of molecule adsorption onto surfaces to chemical kinetics of reactions that happen on catalyst surfaces [18, p. 469-475]. Since methylene blue decomposition happens primarily on a surface of a catalyst - $TiO_2$ as examined in this work, it follows Langmuir-Hinshelwood mechanism as well.

For the specific case of methylene blue photodecomposition on $TiO_2$ surface, the reaction is three-step: adsorption of methylene blue, creation of photogenerated holes/$OH\cdot$ radicals and the decomposition reaction itself. At equilibrium adsorption (and keeping other parameters constant), the reaction rate is linearly dependent on the surface site coverage

$\theta_{MB}$ - the amount of catalyst surface sites that are occupied by methylene blue [18]:

$$Rate = k\theta_{MB} \tag{3.1}$$

The constant $k$ is directly related to the efficiency of the catalyst, as it shows how fast methylene blue decomposes on it's surface. According to Langmuir's adsorption theory, $\theta$ for a single reactant A at equilibrium follows the so-called Langmuir isotherm [18, p. 470]:

$$\theta_A = \frac{K[A]}{1 + K[A]} \tag{3.2}$$

where $[A]$ is the concentration of the species and $K$ an adsorption-desorption rate constant. For small concentrations of the reactant simplifies to:

$$\theta_A = K[A] \tag{3.3}$$

from which it follows that the decomposition rate for small concentrations of methylene blue is proportional to concentration:

$$Rate = kK[A] = \frac{d[A]}{dt} \tag{3.4}$$

From that we can derive the equation for the MB concentration in solution $c$ during decomposition with the apparent rate constant $k_{app} = kK$ and initial (equilibrium) concentration $c_0$ as parameters:

$$c = \int -Rate\, dt = \int -k_{app} c\, dt = c_0 e^{-k_{app} t} \tag{3.5}$$

The negative sign before $Rate$ is added since the rate is derived for the decomposition reaction. To continue to practical considerations for catalyst evaluation, efficiency of the catalyst will be correlated with the rate constant $k$ of decomposition and therefore $k_{app}$. However, different catalysts will also have varying initial concentrations $c_0$ since different amounts of methylene blue will be adsorbed onto the catalyst surface, which in itself is not correlated with efficiency. Therefore, we can modify the equation 3.5 to normalise the concentration with respect to its value at the start of light exposure (decomposition) $c_0$:

$$\frac{c}{c_0} = e^{-k_{app} t} \tag{3.6}$$

The impact of the value of $k_{app}$ on the shape of the resulting normalised curve is shown in the following Figure 3.4.

The shape of the photodecay concentration curve will therefore be directly correlated with

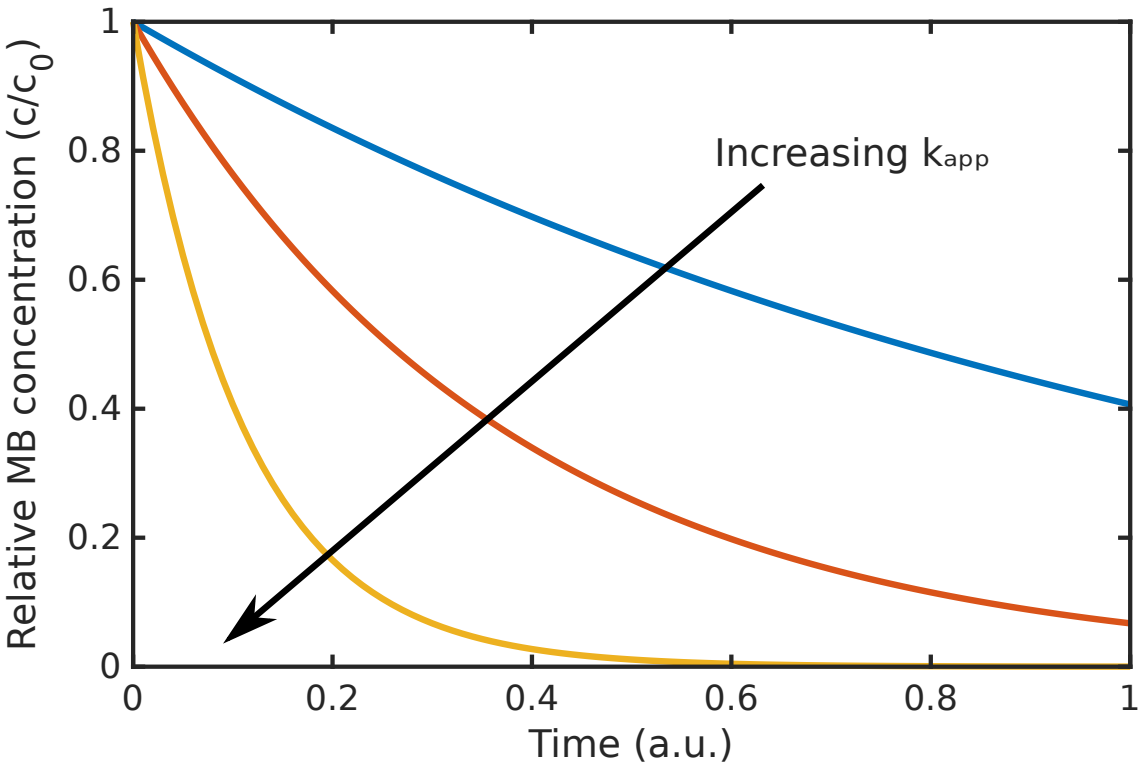


***Figure 3.4.*** *Photodecay concentration curves according to Langmuir-Hinshelwood mechanism for different values of $k_{app}$ in equation 3.6*

the photocatalyst efficiency: photocatalysts with higher photocatalytic efficiency will have steeper curves than those with lower efficiency, which allows us to compare different photocatalysts in this work.

Furthermore, it is possible to derive $k_{app}$ from the normalised concentration data:

$$-ln\left(\frac{c}{c_0}\right) = k_{app}t, \tag{3.7}$$

therefore by plotting $-ln\left(\frac{c}{c_0}\right)$ against $t$ the gradient of the resulting curve will be $k_{app}$. As discussed above, $k_{app}$ directly correlates to the efficiency of the photocatalyst and can be therefore be used to quantitatively compare said photocatalysts.

Finally, it is important to note that the kinetics of the reaction depend on the amount of methylene blue that is adsorbed on the surface of the photocatalyst, and the above equations have been derived for methylene blue adsorption-desorption equilibrium. Literature sources for methylene blue adsorption kinetics on $TiO_2$ show that a period of equilibriation of at least 60 minutes with the solution stirred in the dark before light exposure is required [6].

# 4 SPECTROPHOTOMETRY

Spectroscopy is the branch of science that is concerned with measurement of the emission and absorption spectra of light and other forms of electromagnetic radiation [12]. Spectrophotometry is a more specialised area of spectroscopy which studies interaction of matter with light in visible, near-infrared and near-ultraviolet wavelength ranges. There is a number of processes that can occur in interaction of radiation with matter: absorption, scattering, reflection, fluorescence, phosphorescence and photochemical reactions [3, p. 13]. Spectrophotometry is specifically suited for measurements of transmittance or how much light of specific wavelengths passes through a sample, reflectance or how much light of specific wavelengths is reflected from a sample and through those - absorptance - how much light of specific wavelengths is absorbed a sample.

In this chapter, basics of spectrophotometer design, measurements that are possible with such devices as well as their applications are discussed.

## 4.1 Working principles and design of a spectrophotometer

Spectrophotometer is a device that measures the trasmittance, reflectance and absorbance of a sample as a function of the wavelength of electromagnetic radiation used. The basic design of a conventional single-beam spectrophotometer is shown in Figure 4.1.

The first major part of a spectrophotometer is a broadband light source, which is responsible for creating the electromagnetic radiation used for the measurement. Depending on the target wavelength range, differing sources are used. For measurements in near-UV and short-wavelength visible light range deuterium arc lamps are often used. A typical

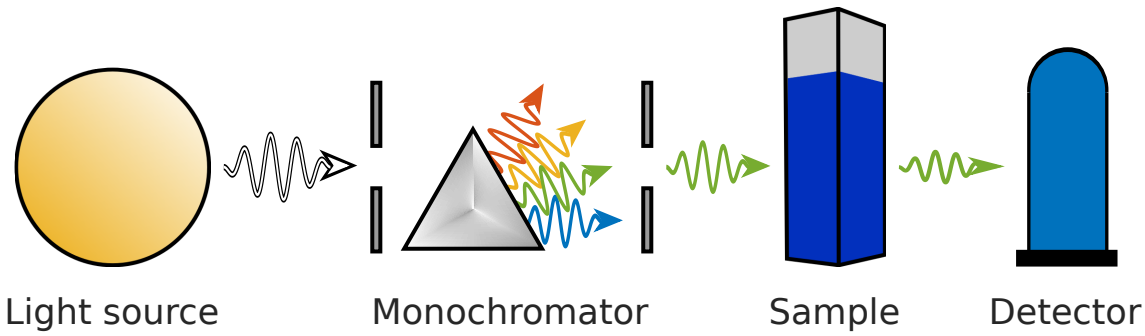


***Figure 4.1.*** *Basic design of a conventional single-beam spectrophotometer, adapted from [3, p. 47]*

second light source to extend the range to visible and near-infrared is a tungsten-halogen lamp. In some instruments xenon lamps are used for their high intensity across the entire visible range, but their higher noise precludes their active use in precision instruments [3, pp. 31-32].

The next component in the light path of a spectrophotometer is a monochromator, which converts the broadband light of the light source to light of a variable narrow wavelength range used for measurement. The simplest and historically first way to monochromate light is by using a prism, made out of glass or another optically transparent material. Prism monochromators, however, have one important disadvantage - the wavelength dispersion they produce is highly nonlinear and sensitive to temperature variation [3, pp. 32-33]. For that reason, most modern spectrophotometers use holographic grating monochromators, which use glass substrates with very narrow grooves photopatterned onto them. The gratings are subsequently coated with a highly reflective material, i.e. aluminium, to form the final grating. When wideband light is shined on such a grating, light is reflected at different angles with respect to wavelength (dispersed). Holographic gratings produce a very linear angular wavelength dispersion. A complete monochromator includes an entrance slit, an exit slit and a dispersion device. An ideal monochromator would produce purely light of a single wavelength, but in practice the wavelength distrubution of exiting light is defined by the shape and dimensions of the slits [2, pp. 29-33].

After monochromation, the light is passed through the sample and after that its intensity is measured with the help of a detector. Several types of detectors are applicale for measurement of different wavelength ranges. One common detector type is a photodiode. In a photodiode, light falls on a photosensitive semiconductor material, which absorbs the light to create free charge carrier pairs and therefore allows current to flow. The amount of free charge carriers created and therefore the photodiode current is linearly related to light intensity. The wavelength range of a photodiode depends on the semiconductor material used, but they typically span UV to near-IR. Another detector type commonly used in spectrophotometers is photomultiplier tube. Photomultiplier tubes combine light detection with several stages of amplification, which allows them to have high sensitivity [3, pp. 33-34]. The wavelength range of a photomultiplier tube depends on the phosphor used for the detector cathode, but can be as wide as UV to near-IR [2, p. 97]. More specialized detectors are available for other wavelength ranges.

## 4.2 Practical applications of spectrophotometry

As noted before, spectrophotometry is most suitable for transmittance, reflectance and absorptance measurements. Such measurements allow determination of many related material properties. Since electronic transition energies of many materials lie in the same energy range as photon energies of light in UV and visible wavelength ranges, it is possible to study electronic properties of different materials through spectrophotometric measurements [4, p. 49]. For example, by measuring absorptance of a sample and applying

Tauc-Lorentz model to the measurement results, it is possible to determine the optical bandgap of the measured material. Knowledge of the bandgap is important for instance in research on photocatalytic materials for water splitting, because it determines the details of photocatalytic reactions in presence of sunlight. Depending on the design of the spectrophotometer in use, differentiation of specularly (directly) reflected light and diffusely scattered light (scattered from the surface of the sample) may be possible. Diffuse reflectance measurements allow for determination of bandgap of samples that do not have significant light transmission through an adapted version of Tauc-Lorentz model [4, p. 57-60]. Furthermore, through measurements of absorption of light in the IR wavelength range it is possible to determine material composition. Different types of chemical bonds correspond to different vibrational energy levels, which in turn correspond to different absorption peaks in the IR range [19, pp. 398-402]. In addition, many biochemical applications exist for spectrophotometry. For example, reactant that changes colour in presence of an enzyme can be added to an enzymatic sample, and through light absorption measurements the exact concentration of the enzyme can be derived.

# 5 LASER TRANSMISSION MEASUREMENT

Despite it's flexibility, spectrophotometry has downsides which give an opportunity for alternative methods of measuring light transmittance to arise. Such downsides include: long aquisition times, large amounts of potentially unnecessary data generated, and simply the expense of maintaining and managing such a complex instrument. A convenient alternative, specifically suitable for methylene blue concentration determination is laser transmission measurement, where light transmission is measured very quickly at the specific laser wavelength. The details of the method are discussed in this chapter.

## 5.1 Laser transmission measurement

The setup for laser transmission measurement is, in its essence, a simplified version of a single-beam spectrophotometer and is shown in Figure 5.1. The light source and monochromator are replaced with a collimated laser of fixed wavelength, foregoing wavelength adjustability for stability and simplicity. The light is then passed through the sample, and its attenuation is measured with help of a detector. In this work, the detector type used is a Si photodiode, where the measured photodiode current is proportional to illumination intensity [20]. The proportionality constant is dependent on the wavelength of illuminating light, which is fixed in case of laser light. For the specific case of methylene blue concentration measurement, a laser in the range of the main absorption peaks of methylene blue - 550 - 700 nm is required. As previously discussed in section 2.2, Beer's law allows us to determine concentration of a desired substance by measuring the light intensity in absense and presence of a sample, based on a set of coefficients deter-

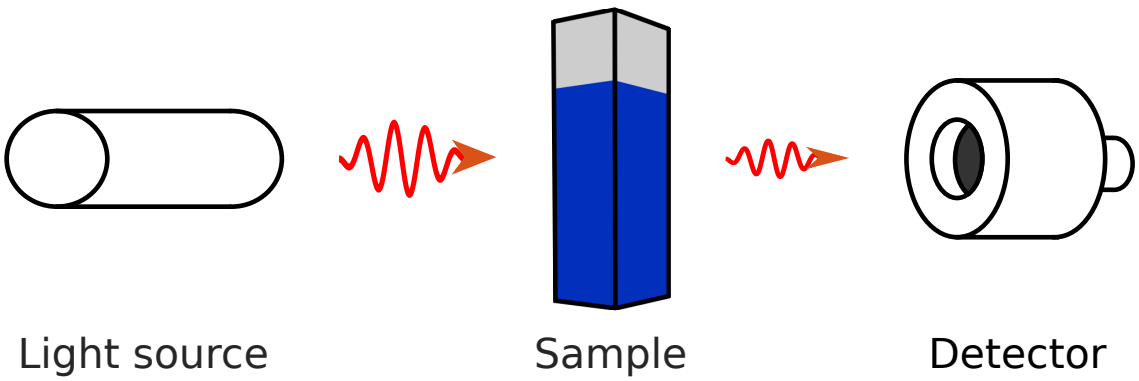


***Figure 5.1.*** *Diagram of a laser transmission measurement setup as used in this work*

mined by measuring a series of samples of known varying concentration. Since with a Si photodiode photodiode current is proportional to illumination intensity we can substitute corresponding currents in lieu of intensities in Beer's law, which simplifies the calculation of the results.

# 6 RESEARCH METHODOLOGY AND EQUIPMENT

The materials used in this work have been prepared at the premises of Surface Science Laboratory of Tampere University, and measured with equipment situated at the premises of Surface Science Laboratory and Photonics Research Community of Tampere University. This chapter examines catalyst materials used in the work, light exposure, spectrophotometric and laser transmission measurement setups as well as experimental methods of the work.

## 6.1 Catalyst materials

The basic structure of the catalysts used in this work is shown in Figure 6.1.

The catalysts under consideration are of core-shell subtype. The catalysts are based on the core of BCR-066 QUARTZ reference particles (European Commission Joint Research Centre, Institute for Reference Materials and Measurements), which have a median (Stokes) diameter of 1.12 $\mu$m [21]. The BCR particles have been functionalised with a coating of 30 nm of $TiO_2$ in PICOSUN TM R-200 Advanced ALD reactor, for $TiO_2$ proportion of 19.7 wt. %. The coating was grown from tetrakis(dimethylamino)titanium (TDMAT) and DI water precursors with argon carrier gas at temperatures of 100°C and 200°C. After growth, the catalysts were subject to a rapid thermal annealing (RTA) treatment in a tube furnace at 500°C for 47 minutes total - 2 min for heating and temperature stabilisation and 45 min for annealing. The photocatalyst samples used in this work are listed in Table 6.1. In the preliminary stages of this work, a pure $TiO_2$ particulate catalyst (Sigma-Aldritch product code 718467-100G) was used to establish the methods in use in the work. The particle size of aforementioned catalyst is on average 21 nm.

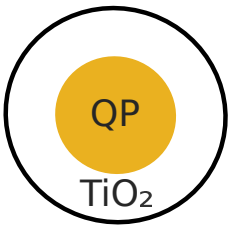


***Figure 6.1.*** *ALD $TiO_2$ on BCR QUARTZ particles core-shell catalyst structure*

***Table 6.1.*** *Photocatalyst samples used in this work*

| | Sample | $TiO_2$ growth temperature | Annealing temperature |
|---|---|---|---|
| q | TiOx 30nm/QP 100C RTA 500C | 100 °C | 500 °C |
| | TiOx 30nm/QP 200C RTA 500C | 200 °C | 500 °C |

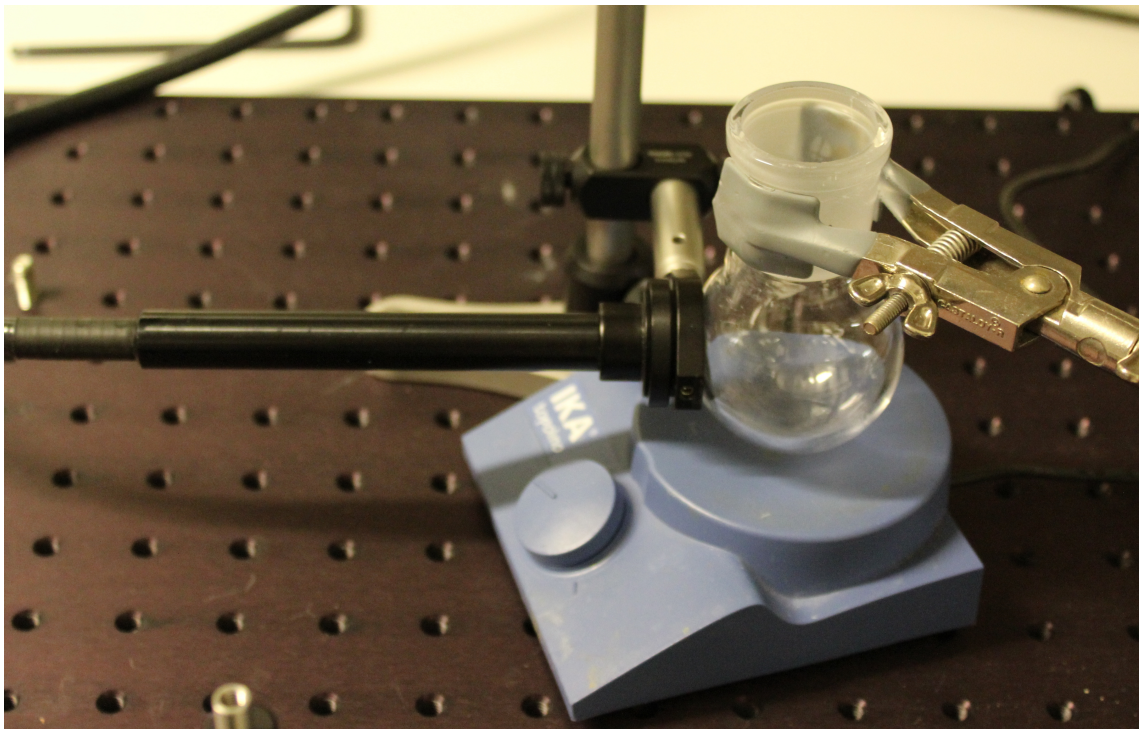


***Figure 6.2.*** *Light exposure experimental setup*

## 6.2 Light exposure

For light exposure a custom setup was developed at the Surface Science Laboratory and is shown in the following figure 6.2.

The centerpiece of the exposure setup was the Electro-Lite Corporation ELC-800 UV light system. The end of the light guide directing the light from the source to the flask with solution (left) was fixed at 3 mm from the flask, centered with respect to spherical part of the flask. Illumination power of the light source was constant at 7.9 W during the experiments, according to the internal sensor. It is important to note that that does not correspond to the power received by the catalyst, as a fraction of the light from the source is scattered by the catalyst or transmitted through the solution and flask and in addition the liquid level changes as samples are taken from the flask so the relative power increases during the course of experiment. The following parts of the exposure setup are the quartz round-bottom flask where the solution is held (right top), the PTFE magnetic stirring bar and magnetic stirrer to agitate the solution and keep catalyst from settling (right bottom). Finally, the setup was contained in a cardboard enclosure (not shown) for preventing external light from influencing the exposure.

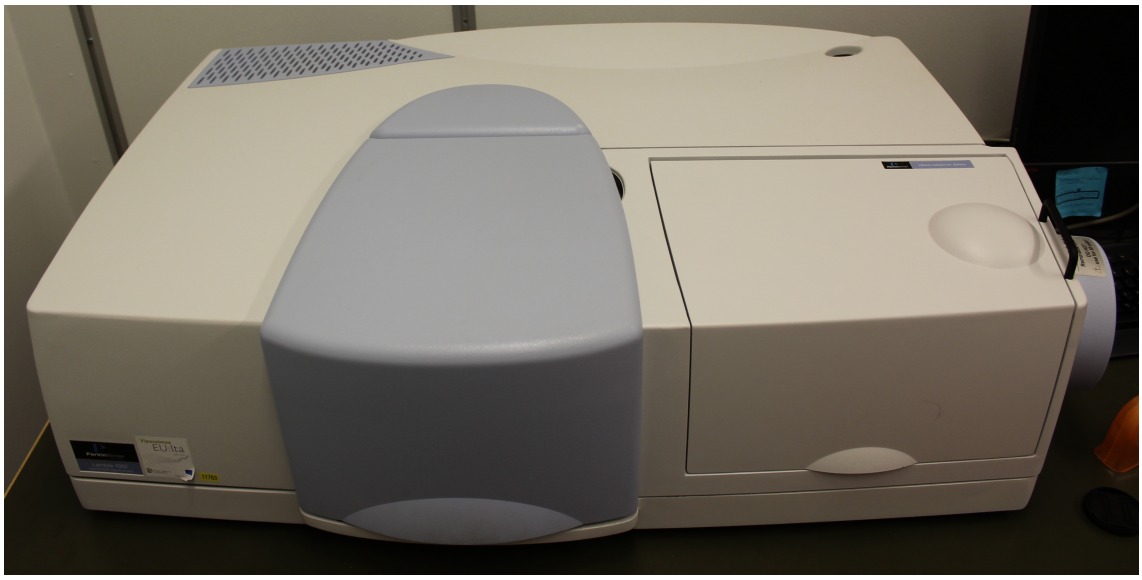

***Figure 6.3.*** *PerkinElmer LAMBDA 1050 UV/Vis/NIR spectrophotometer with the Integrating Sphere module*

## 6.3 Spectrophotometer

Spectrophotometric measurements were performed on the PerkinElmer LAMBDA 1050 UV/Vis/NIR spectrophotometer. The spectrophotometer uses a combination of a deuterium lamp and a tungsten-halogen lamp. For monochromation, the instrument utilises two holographic gratings. If desired, light can be attenuated or polarised after monochromation [22]. For holding the sample in the light beam path a cuvette holder accessory was utilised. The instrument has a modular detection architecture, and in this work the Integrating Sphere module was used, as seen in Figure 6.3. The Integrating Sphere module contains a 150 mm Spectralon® Integrating sphere with two detectors - Extended Range PMT for measurements in 175 nm to 860 nm wavelength range and PbS conductivity detector for measurements in 860 nm to 2500 nm wavelength range. The construction of the Integrating Sphere allows for direct measurement of transmittance, reflectance and diffuse reflectance [23].

LAMBDA 1050 is a digital instrument, where the measurement parameters, such as desired range of measured wavelength, sampling interval, monochromator slit dimensions, etc. are configurable with a computer and measurement results are retrieved directly in digital form. For the purpose of this experiment the following key parameters were used: changeover from the deuterium lamp to the tungsten lamp at 319 nm, wavelength range 800.00 to 250.00 nm, data interval 2.00 nm, measurement cycle time 1.0 s, monochromator changeover at 860 nm, monochromator slit fixed at 2.00 nm, common beam mask 10%.

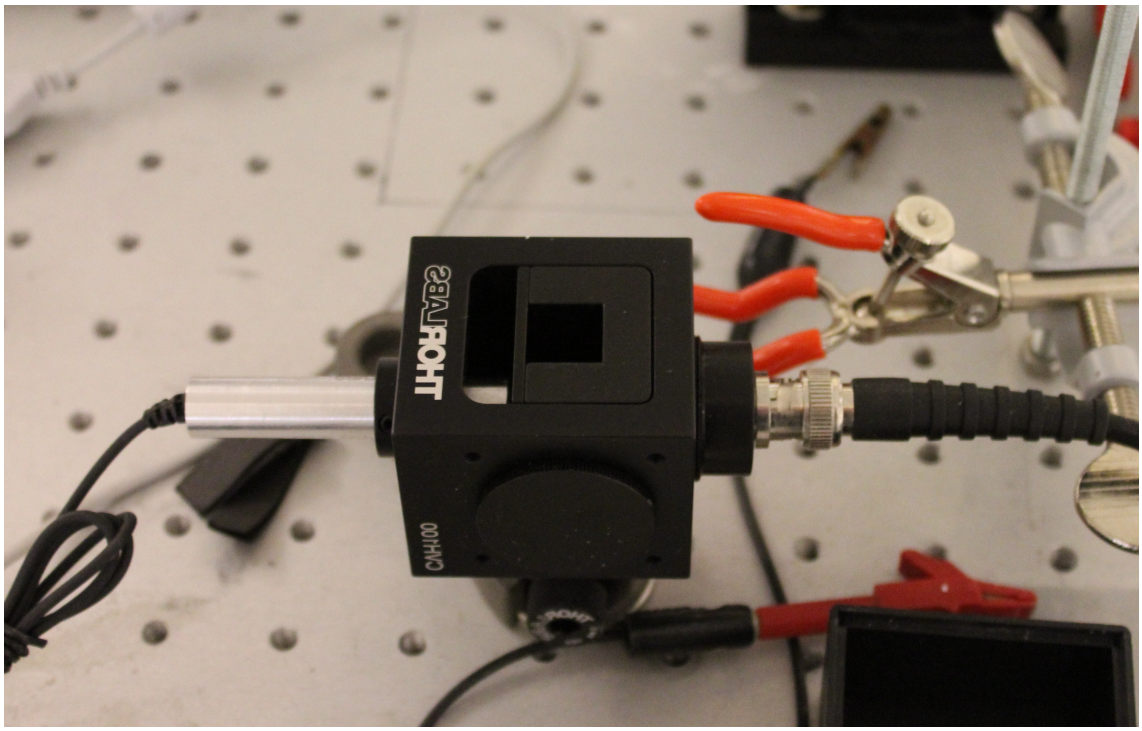


***Figure 6.4.*** *Laser transmission measurement experimental setup*

## 6.4 Laser transmission

For laser transmission measurement a custom setup was developed at Surface Science Laboratory and is shown in the following figure 6.4.

The laser source for this setup is on the left in the figure - the ThorLabs CPS635R Collimated Laser Diode Module, emitting 1.2 mW in a narrow band centered at 635 nm [24]. The detector used is the ThorLabs SM1PD1A Mounted Silicon Photodiode (on the right in the figure), with detection range of 350 to 1100 nm [20], supported by ThorLabs PDA200C Benchtop Photodiode Amplifier for photodiode current measurements. The laser source and the detector were attached to a ThorLabs CVH100 cuvette holder (in the center) with appropriate adaptors, resulting in a stable measurement setup. It must, however, be noted that acrylic cuvettes often differ in size from the holder socket and if a cuvette is permitted to rotate in the holder the path length changes measurably. For stabilisation of cuvette position in the holder, shims have proven an effective method. The cuvette holder includes a lid (not shown) to prevent external light from influencing the measurement.

## 6.5 Procedure

After preparation of the exposure setup described above, 50 ml of DI water (from a Millipore Milli-Q unit) was introduced to the round-bottom flask with 15.1 mg of the $TiO_2$ on quartz particles powder (60 ppm $TiO_2$ loading), as well as 0.2 ml of 0.05 wt.-% aqueous solution of methylene blue (Sigma-Aldritch product code 319112-100ML) (2 ppm MB concentration in solution). The enclosure was placed on top and left for equilibriation (in

the dark, stirring) for 90 min. Then light exposure was done in intervals of 15 min and samples of 3 ml taken at same intervals to centrifuge tubes and left in a dark container until further processing. Total exposure time was 90 min. After exposure, samples were processed for further measurements. First, they have been put into an Hermle Z 233 M2 centrifuge for 10 min at 7000 G loading to separate the catalyst from the methylene blue solution, then 2 ml of each sample was decanted to an acrylic cuvette for measurement. The acrylic cuvettes utilized in this work have a light path length of 10 mm.

After exposure and processing, samples were measured with the laser transmission setup and/or the spectrophotometer. Laser transmission measurements the measurements were performed in the following fashion. The photodiode current with no cuvette in place was first recorded. Then samples were inserted in turn and photodiode current with sample in place was recorded. Spectophotometric measurements were performed in a similar fashion. First the 100% transmission baseline was measured with no sample in place, then sample cuvettes were inserted and measured in turn.

# 7 EXPERIMENTAL RESULTS AND ANALYSIS

In this chapter the results of measurements as described in chapter 6 are presented, analysed and discussed.

## 7.1 Acrylic cuvette transmittance

To begin with, transmittance spectra of various cuvettes were measured on their own. That is crucial for decoupling the absorbance of methylene blue from the absorbance of the cuvette it is contained in as well as the DI water it is dissolved in. The results from acrylic cuvettes used in this work are presented in the Figure 7.1. From the spectra it can be noted that acrylic cuvettes have high transmission all throughout the visible range, however soon after transition into ultraviolet the transmission drops radically. That is generally in line with literature information for light absorption in acrylic plastics, taking into account the fact that exact formulation for these particular cuvettes is not released by the manufacturer. The light transmission through the cuvette is also influenced by the Fresnel (reflection) losses at the acrylic-air interfaces due to their large refractive index difference. That is highlighted in the graphs by the fact that transmittance actually increases when the DI water is added to the cuvette, since the refractive index difference between water and acrylic is much lower than acrylic and air. In addition, DI water does contribute some absorbance in the measured spectra, seen i.e. in the small transmittance drop at approx. 700 nm. Now that the cuvette + DI water transmittance in the wavelength range of interest has been determined and analysed, it has been substracted (in absorbance form) from the spectra that follow in this chapter.

## 7.2 MB solution absorbance after photodecay

As it has been discussed in the theory sections, MB absorbance should be linearly dependent on its concentration in solution. However, when preliminary work has been done in developing the experimental setup of this work results diverging from the theoretical expectations were seen. In the following figure 7.2 absorbance spectra of an MB solution after photodegradation with pure $TiO_2$ particulate catalyst are shown: As it can be clearly seen in the figure, as the photodecomposition progresses, the shape and position of the main methylene blue absorption peak and the methylene blue dimer peak change quite drastically (hypsochromic effect). The shape and position of the secondary MB absorption peak at 290 nm, however, barely see any change. The absorption does decrease

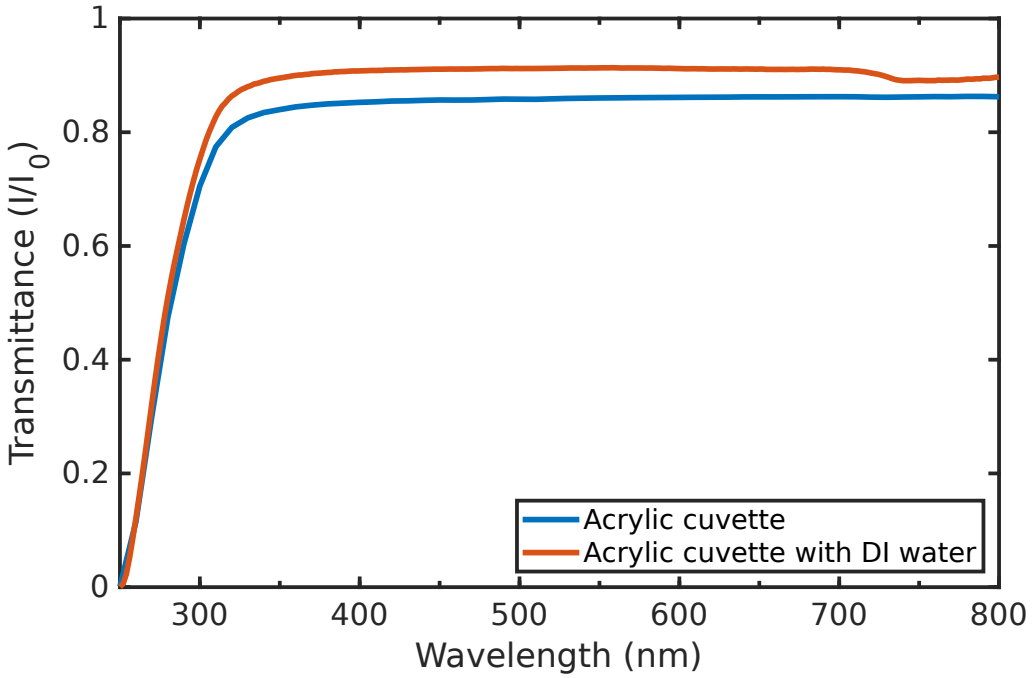


***Figure 7.1.*** *Transmittance spectra of an acrylic cuvette, with and without deionized water*

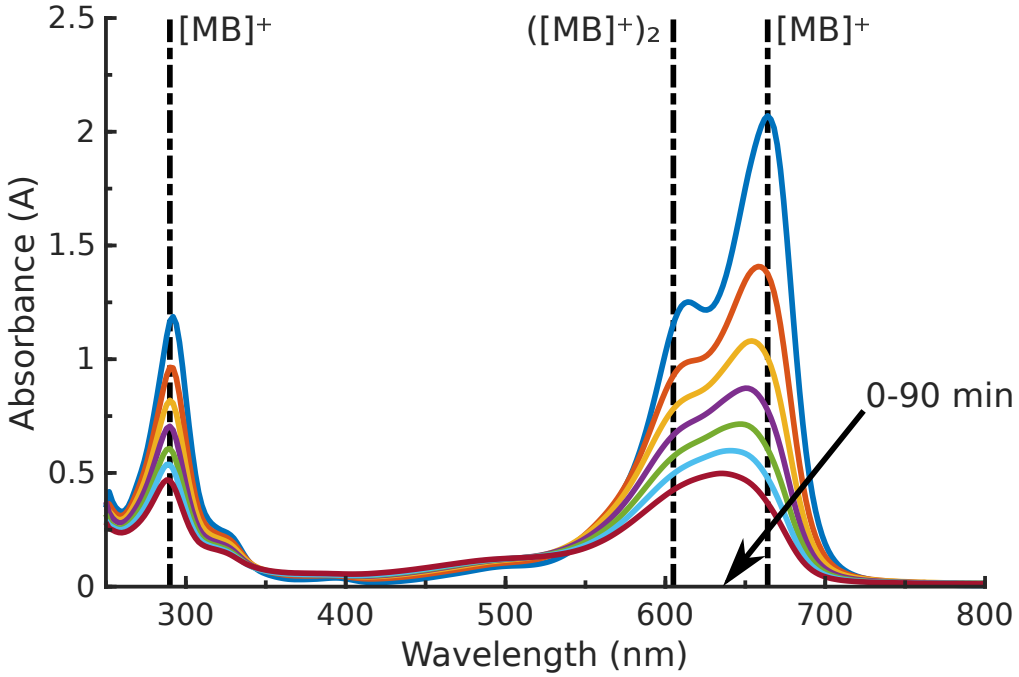


***Figure 7.2.*** *Absorbance spectra of an MB solution after photodegradation with the pure $TiO_2$ catalyst*

across the spectra as the light exposure time decreases, which strongly suggests that photodecomposition is taking place. Author's attempts to eliminate the effect - thorough cleaning of the entire photodecomposition setup, change of the photocatalyst, change of stirring bar, change of the light source and methylene blue bottle to a fresh one, etc. - were ultimately fruitless. Unfortunately, that places investigation of the root cause of the effect outside the scope of this work. Author suggests that the possible cause of the effect may be intrinsic to the methylene blue source used. The purity of the methylene blue is not explicitly specified by the manufacturer, but from the analytic grade and other methylene blue offerings of the manufacturer can be expected to be greater than or equal to 97%. As methylene blue concentrations in use are small - 2 ppm and under, even a small amount of impurity could have an effect on the spectra, since as noted in theory section they are highly sensitive to the environment. An impurity could interact with the methylene blue decomposition products, of which a large number exists, and create a species that interferes with methylene blue or intrinsically has absorption in the wavelength range of the main MB absorption peak. It is possible that the catalyst material itself is the cause of the effect, i.e. hypsochromy has been observed in MB solution photodecay with $BiVO_4$ photocatalysts [25], however deeper investigation would be required to support that conclusion.

Since the shape and position of the secondary MB absorption peak at 290 nm stay appreciably constant, the absorbance in that range can be used for determination of MB concentration instead of the main peak. An experimental run was taken and measured with both spectrophotometer and the laser transmission setup, concentration of methylene blue for each sample was determined from comparing absorbance at the 290 nm peak to that pure MB (Figure 3.2), and dependence of absorbance at 636 nm in the laser setup on concentration was determined, as seen in Figure 7.3. As shown in the figure, despite the dependence of absorbance on concentration slightly deviating from linear it is still sufficiently close to linear to be able to approximate it as such for the purpose of this work. The consequences of the approximation shall be described in more detail in 7.3. The coefficients $k$ and $k * A_0$, as discussed in 2.2, were then determined from the linear fit and used to determine the MB concentration in the following experimental runs.

## 7.3 ALD $TiO_2$/QP catalyst measurements and analysis

Light exposure and laser transmission measurement experiments were then performed to the ALD $TiO_2$ on QP samples. In addition, an experimental run without any catalyst added to methylene blue was performed. Methylene blue concentration was then determined from the photodiode current readings with the coefficients as determined in section 7.2 and the results are shown in Figure 7.4. From the spectra in the figure, a number of observations can be made. To begin with, the starting concentration at 0 min light exposure is below the 2 ppm set up before the 90 min equilibriation, and the sample with no catalyst has the highest concentration. That is as expected, since some amount of methylene blue would be adsorbed on the surface of the catalyst as well as the flask

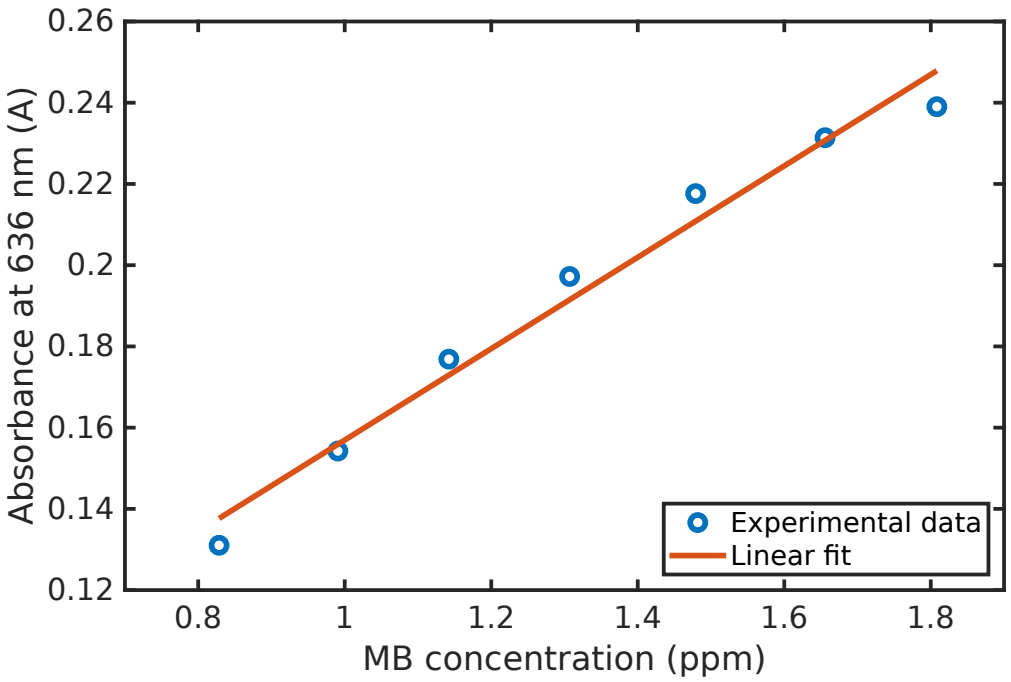


***Figure 7.3.*** *Absorbance of light of wavelength 636 nm in MB solution after photodegradation versus MB concentration. MB concentration derived from 290 nm secondary peak using full absorbance spectra measured with the spectrophotometer*

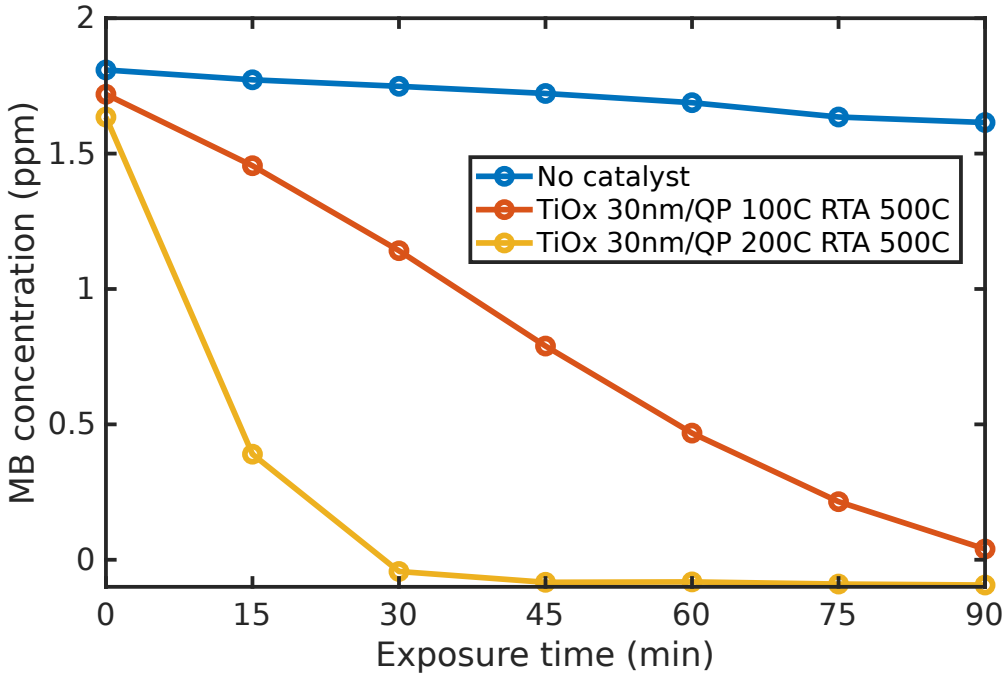


***Figure 7.4.*** *MB photodecay absolute spectra*

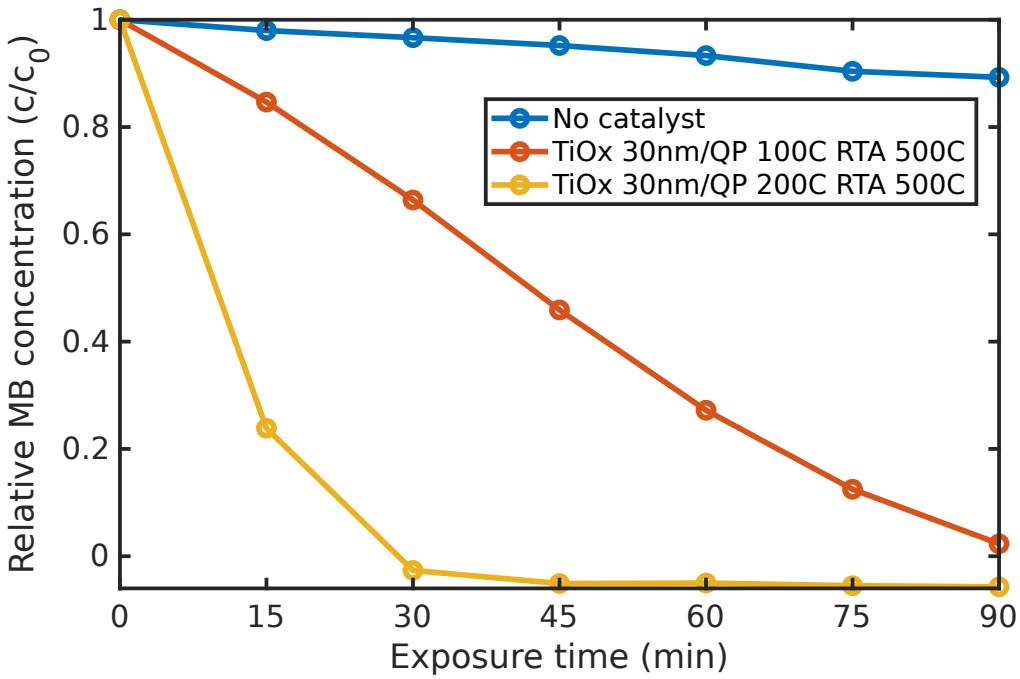


***Figure 7.5.*** *MB photodecay relative spectra*

containing the solution, and the amounts adsorbed will vary among the catalysts.

Secondly, the final concentration for the $TiO_2$ 30nm/QP 100C RTA 500C experimental run is consistently below 0 ppm at approx. -0.06 ppm. This can be considered the aforementioned consequence of the approximation we've taken in section 7.2 when determining the coefficients for determining the methylene blue concentration. First of all, we have approximated a non-linear absorbance-concentration curve as linear, and secondly, we have extrapolated the curve from the approx. 0.8 to 1.8 ppm range in Figure 7.3 to approx. 0 to 1.8 ppm range in Figure 7.4. The magnitude of the final error, assuming complete methylene blue decomposition for final concentration of 0 ppm, is then 0.06 ppm, which is significant. A suggested future improvement to the experimental protocols described in this work would then be usage of a calibration run with larger range for determining the coefficients in the methylene blue concentration to absorbance relation, as well as implementing a true non-linear model for dependence of the two aforementioned quantities. Alternatively, a simplified version of the method can be established, decreasing the exposure time so that the range of methylene blue concentration change is smaller and the concentration is kept in the range where the absorption is expected to be sufficiently linear to improve the accuracy of the analysis.

As discussed in 3.3, due to varying amount of methylene blue adsorbed on the surface of the catalysts compared, a change in concentration relative to initial concentration is a better metric for comparing catalysts than simply absolute concentration change. The data of Figure 7.4 normalised in such fashion is shown in Figure 7.5. As we can see from the figure, the different experimental series are easily distinguishable from one another. As it has been discussed previously, MB slowly photolyses with light exposure in absense

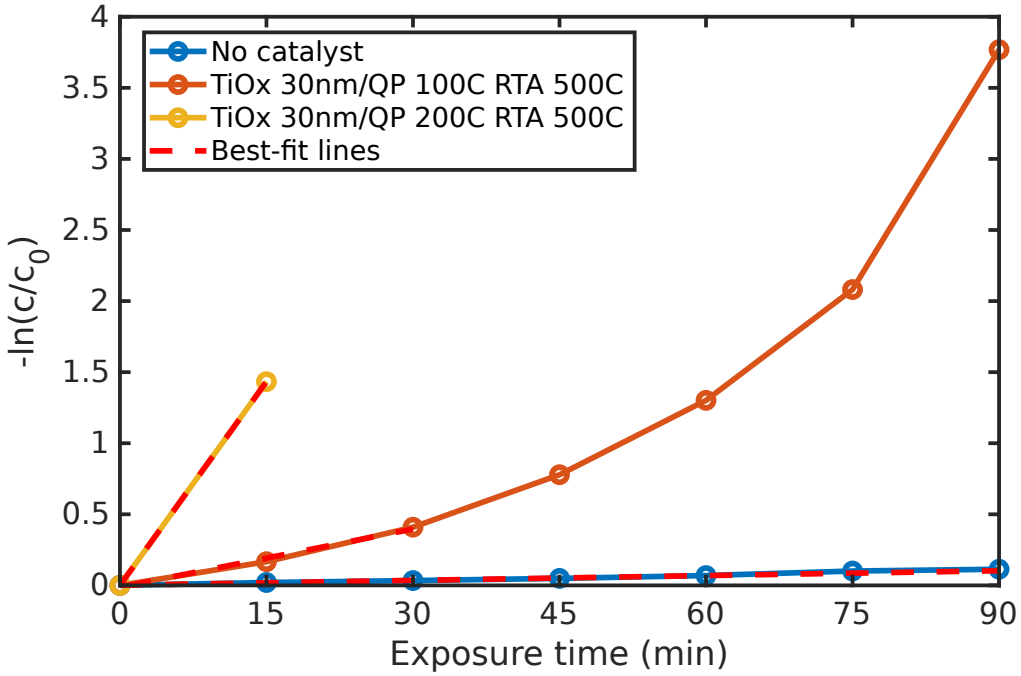


***Figure 7.6.*** *Determination of $k_{app}$ from concentration data*

***Table 7.1.*** *Results of $k_{app}$ derivation*

| Sample | $k_{app}$ |
|---|---|
| No catalyst | $1.1 * 10^{-3} min^{-1}$ |
| TiOx 30nm/QP 100C RTA 500C | $13.6 * 10^{-3} min^{-1}$ |
| TiOx 30nm/QP 200C RTA 500C | $95.6 * 10^{-3} min^{-1}$ |

of catalyst [15], which is confirmed in this experiment as the relative MB concentration slowly decreases as exposure continues. Presence of the catalyst causes much faster decomposition to take place. The shape of the relative concentration curve follows the expected exponential-like decrease. The catalyst material with $TiO_2$ grown at 200 °C appears to possess a significantly higher photocatalytic activity than $TiO_2$ grown at 100 °C since for catalyst with $TiO_2$ grown at 200 °C the MB decomposition curve is much more steep than one with $TiO_2$ grown at 100 °C.

Furthermore, as discussed in 3.3 we can use the concentration data to derive $k_{app}$ by plotting $-ln\left(\frac{c}{c_0}\right)$ against time and finding the gradient of the curve, as shown in Figure 7.6. For the catalyst sample with $TiO_2$ grown at 200 °C the range of investigation had to be limited to first 15 min of the decomposition since after that the calculated values for concentration turn negative due to reasons outlined above and natural logarithm is defined only for non-negative real numbers. For catalyst material with $TiO_2$ grown at 100 °C the curve appears to deviate significantly from linear, which is why $k_{app}$ was derived from first 30 min, as in that time range the concentration stays in the 0.8 to 1.8 ppm range (as seen in Figure 7.4) which we have derived calibration values from (Figure 7.3) and so have the greatest accuracy in. The results for $k_{app}$ are shown in the following Table 7.1.

The results of $k_{app}$ determination as per Table 7.1 mirror the quantitative results of Figure 7.5. The apparent rate constant value for photodecomposition in absense of photocatalyst is low, 13 times lower than even the least effective of the photocatalysts. The catalyst material with $TiO_2$ grown at 200 °C is more photocatalytically active than $TiO_2$ grown at 100 °C by a large margin, with 600% higher apparent methylene blue photodecomposition rate.

# 8 CONCLUSION

In this work, method for evaluation of performance of novel photocatalysts based on photodecomposition of methylene blue has been established. The theoretical foundations behind methylene blue decomposition measurements have been reviewed, and the method described. In this work, methylene blue main absorption band position and shape shifted during the decomposition, which does not completely follow the theoretical foundations outlined in the work. However, on closer analysis it has been shown that photodecomposition is indeed taking place, and a method outlined to derive methylene blue concentration in solution despite the non-linear decomposition profile.

The final model for methylene blue decomposition shows reasonable agreement with theory. Initial methylene blue concentration shows signs of adsorption onto catalyst surface, and the decomposition profile is as L-H reaction mechanism predicts that of an exponential decrease. Catalysts under evaluation are clearly distinguished from each other, allowing the desired comparison between their activities which the method is designed to show. Core-shell catalyst with $TiO_2$ ALD grown at 100 °C is shown to have significantly lower photocatalytic efficiency than one with $TiO_2$ ALD grown at 200 °C. However, significant error is clearly present in the low concentration range, which can in future work be eliminated by improving the calibration data set used to relate absorbance at 635 nm to methylene blue concentration. Furthermore, in future work the source of nonlinearity in the decay spectra themselves couold be identified and eliminated, providing higher quality of data. To conclude, the method outlined in this work could effectively be used for quantitative comparison of photocatalyst activities of novel photocatalysts and be used in research and development of photocatalyst materials.

# REFERENCES


[1] *A Dictionary of Physics*. Oxford University Press, 2015. ISBN: 9780198714743.

[2] N. V. Tkachenko. *Optical spectroscopy: methods and instrumentations*. English. 1st. Amsterdam;Boston; Elsevier, 2006. ISBN: 0444521267;9780444521262;

[3] T. Owen. *Fundamentals of modern UV-visible spectroscopy*. Agilent Technologies, 2000, 136.

[4] Z. Chen, T. G. Deutsch, H. N. Dinh, K. Domen, K. Emery, A. J. Forman, N. Gaillard, R. Garland, C. Heske, T. F. Jaramillo, A. Kleiman-Shwarsctein, E. Miller, K. Takanabe and J. Turner. UV-Vis Spectroscopy. *Photoelectrochemical Water Splitting: Standards, Experimental Methods, and Protocols*. New York, NY: Springer New York, 2013, 49–62. ISBN: 978-1-4614-8298-7. DOI: 10.1007/978-1-4614-8298-7_5. URL: https://doi.org/10.1007/978-1-4614-8298-7_5.

[5] A. Iqbal and A. Farrukh. *New Strategies Combating Bacterial Infection*. John Wiley & Sons, 2008, 91.

[6] A. Houas, H. Lachheb, M. Ksibi, E. Elaloui, C. Guillard and J.-M. Herrmann. Photocatalytic degradation pathway of methylene blue in water. *Applied Catalysis B: Environmental* 31.2 (2001), 145–157. ISSN: 0926-3373. DOI: https://doi.org/10.1016/S0926-3373(00)00276-9. URL: http://www.sciencedirect.com/science/article/pii/S0926337300002769.

[7] P. Nuengmatcha, S. Chanthai, R. Mahachai and W.-C. Oh. Sonocatalytic performance of ZnO/graphene/TiO2 nanocomposite for degradation of dye pollutants (methylene blue, texbrite BAC-L, texbrite BBU-L and texbrite NFW-L) under ultrasonic irradiation. *Dyes and Pigments* 134 (2016), 487–497. ISSN: 0143-7208. DOI: https://doi.org/10.1016/j.dyepig.2016.08.006. URL: http://www.sciencedirect.com/science/article/pii/S0143720816303813.

[8] P. Awati, S. Awate, P. Shah and V. Ramaswamy. Photocatalytic decomposition of methylene blue using nanocrystalline anatase titania prepared by ultrasonic technique. *Catalysis Communications* 4.8 (2003), 393–400. ISSN: 1566-7367. DOI: https://doi.org/10.1016/S1566-7367(03)00092-X. URL: http://www.sciencedirect.com/science/article/pii/S156673670300092X.

[9] K. Bergmann and C. T. O'Konski. A spectroscopic study of methylene blue monomer, dimer, and complexes with montmorillonite. *The Journal of Physical Chemistry* 67.10 (1963), 2169–2177. DOI: 10.1021/j100804a048. eprint: https://doi.org/10.1021/j100804a048. URL: https://doi.org/10.1021/j100804a048.

[10] A. G. Zherlitsyn, V. P. Shiyan, L. N. Shiyan and S. O. Magomadova. Destruction of molecular compounds in gaseous and liquid medium in microwave discharge plasma. *Journal of Physics: Conference Series* 652 (Nov. 2015), 012023. DOI: 10.

1088/1742-6596/652/1/012023. URL: https://doi.org/10.1088%2F1742-6596%2F652%2F1%2F012023.

[11] E. Braswell. Evidence for trimerization in aqueous solutions of methylene blue. *The Journal of Physical Chemistry* 72.7 (1968), 2477–2483. DOI: 10.1021/j100853a035. eprint: https://doi.org/10.1021/j100853a035. URL: https://doi.org/10.1021/j100853a035.

[12] C. J. Cleveland and C. Morris. *Dictionary of Energy (Expanded Edition)*. Elsevier, 2009. ISBN: 978-0-08-096491-1. URL: https://app.knovel.com/hotlink/toc/id:kpDEEE0001/dictionary-energy-expanded/dictionary-energy-expanded.

[13] R. Dariani, A. Esmaeili, A. Mortezaali and S. Dehghanpour. Photocatalytic reaction and degradation of methylene blue on TiO2 nano-sized particles. *Optik* 127.18 (2016), 7143–7154. ISSN: 0030-4026. DOI: https://doi.org/10.1016/j.ijleo.2016.04.026. URL: http://www.sciencedirect.com/science/article/pii/S003040261630300X.

[14] H. A. Le, L. T. Linh, S. Chin and J. Jurng. Photocatalytic degradation of methylene blue by a combination of TiO2-anatase and coconut shell activated carbon. *Powder Technology* 225 (2012), 167–175. ISSN: 0032-5910. DOI: https://doi.org/10.1016/j.powtec.2012.04.004. URL: http://www.sciencedirect.com/science/article/pii/S0032591012002355.

[15] D. Dvoranová, V. Brezová, M. Mazúr and M. A. Malati. Investigations of metal-doped titanium dioxide photocatalysts. *Applied Catalysis B: Environmental* 37.2 (2002), 91–105. ISSN: 0926-3373. DOI: https://doi.org/10.1016/S0926-3373(01)00335-6. URL: http://www.sciencedirect.com/science/article/pii/S0926337301003356.

[16] Y. Cong, J. Zhang, F. Chen and M. Anpo. Synthesis and Characterization of Nitrogen-Doped TiO2 Nanophotocatalyst with High Visible Light Activity. *The Journal of Physical Chemistry C* 111.19 (2007), 6976–6982. DOI: 10.1021/jp0685030. eprint: https://doi.org/10.1021/jp0685030. URL: https://doi.org/10.1021/jp0685030.

[17] X. Hong, Z. Wang, W. Cai, F. Lu, J. Zhang, Y. Yang, N. Ma and Y. Liu. Visible-Light-Activated Nanoparticle Photocatalyst of Iodine-Doped Titanium Dioxide. *Chemistry of Materials* 17.6 (2005), 1548–1552. DOI: 10.1021/cm047891k. eprint: https://doi.org/10.1021/cm047891k. URL: https://doi.org/10.1021/cm047891k.

[18] R. G. Mortimer. *Physical Chemistry.* Vol. 2nd ed. Academic Press, 2000. ISBN: 9780125083454. URL: http://search.ebscohost.com/login.aspx?direct=true&AuthType=cookie,ip,uid&db=nlebk&AN=249069&site=ehost-live&scope=site&authtype=sso&custid=s4778523.

[19] P. A. Tipler and R. A. Llewellyn. *Modern physics*. eng. 6th ed. New York: W. H. Freeman and Co, 2012, [61] s. ISBN: 978-1-4292-5078-8. URL: https://tuni.finna.fi/Record/tutcat.256896.

[20] *FDS1010 Si Photodiode Spec Sheet*. Thorlabs, Inc., 2017.

[21] *Certified reference material BCR ® – 066 Certificate of Analysis*. European Commission Joint Research Centre, Institute for Reference Materials and Measurements, 2007.

[22] *Technical Specifications for the LAMBDA 1050 UV/Vis/NIR and LAMBDA 950 UV/Vis/NIR Spectrophotometer*. Perkin-Elmer, 2007.

[23] *LAMBDA 650/750/850/950/1050 Accessories for LAMBDA Series*. Perkin-Elmer, 2012.

[24] *CPS635R Collimated Laser Diode Module Spec Sheet*. Thorlabs, Inc., 2015.

[25] N. C. Castillo, A. Heel, T. Graule and C. Pulgarin. Flame-assisted synthesis of nanoscale, amorphous and crystalline, spherical BiVO4 with visible-light photocatalytic activity. *Applied Catalysis B: Environmental* 95.3 (2010), 335–347. ISSN: 0926-3373. DOI: https://doi.org/10.1016/j.apcatb.2010.01.012. URL: http://www.sciencedirect.com/science/article/pii/S0926337310000263.